

## Hydrothermal reactivity of neutron absorber composites

Journal of Nuclear Materials (short communication)

Kirsten Sauer<sup>1</sup>, Marlena Rock<sup>1</sup>, Florie Caporuscio<sup>1</sup>, Ernest Hardin<sup>2</sup>

<sup>1</sup>Earth and Environmental Sciences, Los Alamos National Laboratory, P.O. Box 1663, MS J966, Los Alamos, NM 87545, sauer@lanl.gov

<sup>2</sup>Sandia National Laboratories, P.O. Box 5800, MS 0779, Albuquerque, NM 87185.

**Keywords:** neutron absorber composite materials, dual-purpose canister, repository, boehmite, hydrothermal

### Abstract

The stability of neutron absorber composite materials at hydrothermal conditions was tested in a series of two-week experiments to mimic spent nuclear fuel disposal. Coupons, composed of boron carbide ( $B_4C$ ) sintered with and encased in aluminum, were increasingly altered in experiments at 150, 230, and 300°C and pressures of 150 bar. Alteration of aluminum to boehmite ( $\gamma-AlO(OH)$ ) and hydrogen gas generation occurred over the range of investigated temperatures, but is most significant at 300°C. The formation of boron-bearing mineral phases was not detected; however, aqueous boron was present in the reaction fluids.

### Main body

Direct disposal of spent nuclear fuel in dual-purpose canisters (DPCs), designed for storage and transportation, is attractive in order to reduce waste, potential worker dose, and cost [1]. Currently, most spent nuclear fuel and waste in the United States is stored at the site of production in DPCs [2,3]. The largest existing DPCs can hold up to 37 pressurized-water or 89 boiling-water reactor assemblies [4]. As a result, DPCs are associated with higher thermal loads than considered by most repository designs (i.e., [5]) and require the inclusion of criticality control materials (i.e., neutron absorber composites).

3M™ Neutron Absorber Composite (formerly known as Boral®) is composed of a core of ceramic-metal composite material composed of 25–250  $\mu m$  boron carbide ( $B_4C$ ) grains sintered with aluminum and clad in aluminum. Boron carbide acts as a neutron absorber, whereas aluminum is a lightweight binding material. The sintered core is ~35–65 vol.%  $B_4C$  relative to aluminum, with and 1–10% porosity.

The ceramic-metal composite is attached to stainless steel plates, and is not structural nor credited for heat rejection. The main concern is the reactivity of aluminum in water, which has been characterized previously [6], and stability of  $B_4C$ . Studies on neutron absorber materials in the presence of moisture have highlighted the corrodibility and blistering of aluminum in a variety of environments (e.g., 7–9). Based on previous studies, aluminum-based neutron absorbers exposed to water may have a lifetime of only 40 years in a disposal scenario [10,11]. Thus, the corrosion of aluminum is expected in the far future within DPCs used for geologic disposal, and needs to be fully characterized to understand the chemical environment within the canister. Therefore, this study explores the hydrothermal reactivity of Neutron Absorber Composite Material (NACM) with deionized water at pressure of 150 bar and a range of temperatures (150–300°C) that may provide insight into material reactions during pre-disposal [12] and repository conditions [5].

Sheets of NACM have a thickness of ~0.3 cm and were cut into rectangular coupons with the approximate dimensions of 1.3 by 3.8 cm (Fig. 1). Hydrothermal experiments with 2–3 coupons were conducted at 150, 230, and 300°C and 150 bar for two weeks (Table S1). Experiments utilized ~150 mL flexible gold reaction cells fixed to a 500 mL Gasket Confined Closure reactor [11,S1], allowing for the extraction of reaction fluids during the experiment. The mineralogy of the reacted composite coupons was characterized with X-ray diffraction (XRD) and scanning electron microscopy (SEM). Fluid compositions were measured using inductively coupled plasma-optical emission and -mass spectrometry (S1). Physical dimensions and SEM characteristics are described in S2.

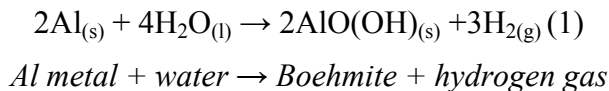
Fluid samples collected weekly and after assembly cooling showed increases in aluminum and boron in solution (Table S2).  $[Al^{3+}]$  increases from below detection in the starting solution to 0.04, 0.4, and ~2 mg/L, with increasing temperature. Boron concentrations reached between 14 and 19 mg/L in all experiments.

Gas generation accompanied extracted reaction fluids and was likely  $H_2$  gas based on the experimental system components. The volume of  $H_2$  extracted (at room temperature and pressure) was estimated to be the following (minimum measured): 1396.0 mL (300°C), 12.6 mL (150°C), and 35.7 mL (230°C).

The main alteration product identified by XRD is (pseudo)boehmite ( $\gamma$ -AlO(OH)), an aluminum oxide hydroxide mineral. Pseudoboehmite is formed in the lower temperature experiment (150°C) and produces broad XRD peaks (Fig. 2a). Boehmite is formed at higher temperature, indicated by sharp, defined peaks (Fig. 2a). Aluminum alteration is pervasive at 300°C and extends throughout the cladding depth at the edges of the coupons based on XRD and SEM observations (Fig. 2b, 3). In the interior of the 230°C and 150°C coupons, aluminum alteration is minimal (Fig. 2b).

The  $B_4C$  peaks show slight changes in shape with higher temperature; XRD peaks in from the 300°C coupons are broad (Fig. 2b), and potentially indicate degradation of the crystal structure. In addition, increased boron concentrations are detected in the reaction fluids (14–19 mg/L), indicating some dissolution (~1% of  $B_4C$  present based on the volume of the reaction vessel and areal density of 0.13 g B/cm<sup>2</sup>).

The NACM coupons included in the experiments experienced physical changes with the most dramatic effects observed in the 300°C experiment (~90% volume and ~54% mass increase, Table 1, Fig. 1). The alteration of aluminum to boehmite is likely responsible for the expansion of the NACM. Coupon expansion and likely associated  $H_2$  gas generation (at least 1400 mL) can be described by the following reaction:



Some hydrogen would be sequestered during boehmite formation, in addition to  $H_2$  generation. For example, assuming all coupon mass gain at 300°C (6.52 g) was due to the addition of -OOH, 0.20 g of H, equivalent to 2.23 L of  $H_2$  gas at room temperature, was sequestered, in comparison to 6.64 L of  $H_2$  gas formed. Therefore, the formation of boehmite is important to consider when calculating the amount of  $H_2$  gas released in NACM hydrothermal reactions.

Material expansion within a canister is also a concern for long-term DPC function. Boehmite formation at 300°C resulted in dramatic coupon expansion over two weeks. Boehmite has a

larger molar volume per mol of aluminum ( $V_m = 19.5 \text{ cm}^3/\text{mol Al}$ ) than aluminum ( $V_m = 10.0 \text{ cm}^3/\text{mol Al}$ ). Thus, based on reaction (1) and  $V_m$  values, the conversion of all aluminum to boehmite would result in a 93% volume increase. The center of the 300°C coupon was observed to be thinner than the edges and unaltered aluminum is present in the coupon core, indicating that aluminum alteration was more prevalent at the porous edges where the composite was directly exposed to water. Thus, boehmite formation, and associated volume expansion, likely opened pathways for fluids to reach the interior of the coupon. The alteration of the aluminum cladding did not form a passivation layer, but rather facilitated progressive boehmite formation from the coupon surface to interior. The amount of aluminum reacted over two weeks at 300°C indicates that likely all aluminum metal would be altered in a relatively short timeframe within a hot waste package exposed to water.

The alteration phase, boehmite ( $\gamma\text{-AlO(OH)}$ ), of the aluminum cladding and sinter of 3M™ Neutron Absorber Composite was identified in a series of experiments replicating spent fuel canister disposal temperature and pressure conditions. The interaction of deionized water and coupons at elevated temperature and pressure caused significant changes to the material physical properties and some dissolution of  $\text{B}_4\text{C}$ , which may affect performance in a disposed spent nuclear fuel canister. Alteration of aluminum cladding and sinter resulted in expansion of the coupon and  $\text{B}_4\text{C}$ -Al composite core. This expansion, likely due to the alteration of aluminum to boehmite results in enlargement of pore spaces and weakening of the composite sinter. Further, hydrogen gas generation occurred, which is a significant concern in dual-purpose canister disposal.

#### **Data availability statement**

Data will be made available upon request.

#### **Declaration of competing interest**

The authors declare that they have no known competing financial interests or personal relationships that could have appeared to influence the work reported in this paper.

#### **Acknowledgements**

This work was funded by the US Department of Energy, Office of Nuclear Energy, Spent Fuel and Waste Disposition Program. Los Alamos National Laboratory has assigned release number LA-UR-19-32409 to this manuscript. Sandia National Laboratories is a multimission laboratory managed and operated by National Technology and Engineering Solutions of Sandia LLC, a wholly owned subsidiary of Honeywell International Inc. for the U.S. Department of Energy's National Nuclear Security Administration under contract DE-NA0003525. Thank you to an anonymous reviewer and Associate Editor Quanying Huang who provided feedback that improved this manuscript.

#### **Disclaimer**

This document was prepared as an account of work sponsored by an agency of the United States Government. Neither the United States Government, nor any agency thereof, nor any of their employees, nor any of their contractors, subcontractors, or their employees, make any warranty, express or implied, or assume any legal liability or responsibility for the accuracy, completeness, or usefulness of any information, apparatus, product, or process disclosed, or represent that its use would not infringe privately owned rights. Reference herein to any specific commercial product, process, or service by trade name, trademark, manufacturer, or otherwise, does not

necessarily constitute or imply its endorsement, recommendation, or favoring by the United States Government, any agency thereof, or any of their contractors or subcontractors. The views and opinions expressed herein do not necessarily state or reflect those of the United States Government, any agency thereof, or any of their contractors.

## References

- [1] Hardin, E.L., Price, L., Kalinina, E., Hadgu, T., Ilgen, A., Bryan, C., Scaglione, J., Banerjee, K., Clarity, J., Jubin, R., Sobes, V., Howard, R., Carter, J., Severynse, T., and Perry, F. 2015, Summary of Investigations on Technical Feasibility of Direct Disposal of Dual-Purpose Canisters (U.S. Department of Energy Office of Used Nuclear Fuel Disposition FCRD-UFD-2015-000129 Rev 0, 2015) 117 p.
- [2] Hardin, E.L., Clayton, D.J., Howard, R.L., Scaglione, J.M., Pierce, E., Banerjee, K., Voegelé, M.D., Greenberg, H.R., Wen, J., Buscheck, T.A., Carter, J.T., Severynse, T., and Nutt, W.M. 2013. Preliminary Report on Dual-Purpose Canister Disposal Alternatives (FY13). FCRD-UFD-2013-000171 Rev. 1. U.S. Department of Energy, Office of Used Nuclear Fuel Disposition.
- [3] Bonano, E.J., Kalinina, E.A., and Swift, P.N. 2018. The Need for Integrating the Back End of the Nuclear Fuel Cycle in the United States of America. *MRS Advances* 3.19: 991-1003.
- [4] Greene, S., Medford, J., & Macy, S. 2013. Storage and Transport Cask Data for Used Commercial Nuclear Fuel. Advanced Technology Insights LLC, Oak Ridge, TN, Technical Report No. ATI-TR-13047.
- [5] Greenberg, H., Wen, J., & Buscheck, T. 2013. Scoping Thermal Analysis of Alternative Dual-Purpose Canister Disposal Concepts. Lawrence Livermore National Laboratory. LLNL-TR-639869.
- [6] K. Wefers and C. Misra. 1987. Oxides and hydroxides of aluminum. ALCOA Laboratories.
- [7] Walters, W.S. 1985. Experimental investigation of corrosion rates and mechanisms in BORAL. *Brit. Corr. Jour.* V2,#2, pp 84-89.
- [7] EPRI. 2010. Experimental Characterization of BORAL® Pore Size and Volume Distributions., Palo Alto, CA. 1021051.
- [8] Wierschke, J.B. 2015. Evaluation of Aluminum-Boron Carbide Neutron Absorbing Materials for interim Storage of Used Nuclear Fuel. Ph.D dissertation, nuclear engineering, University of Michigan.
- [9] Lindquist, K. 2009. Handbook of Neutron Absorber Materials for Spent Nuclear Fuel Transportation and Storage Applications: 2009 Edition. Electric Power Research Institute. Palo Alto, CA. 1019110.
- [10] Ilgen, A.G., Bryan, C.R., Teich-McGoldrick, S., Hardin, E., and Clarity, J. 2014. DPC materials and corrosion environments. United States: N. p., 2014. Web. doi:10.2172/1162055.
- [11] Seyfried, J.R., Janecky, D.R., and Berndt, M.E. 1987. Rocking autoclaves for hydrothermal experiments II. The flexible reaction-cell system. *Hydrothermal Experimental Techniques*. Eds. Ulmer, G.C. and Barnes, H.L. John Wiley & Sons, pp. 216 – 239.

[12] Fort, J.A., Michener, T.E., Suffield, S.R., Richmond, D.J. 2016. Thermal Modeling of a Loaded Magnastor Storage System at Catawba Nuclear Station. No. PNNL-25871. Pacific Northwest National Lab, Richland, WA.

### Figure captions

Fig. 1. Photographs of unreacted and reacted coupons extracted from the hydrothermal experiments highlighting the expansion in three dimensions and changes in physical appearance.

Fig 2. XRD results from the surface (A) and core (B) of reacted and unreacted NACM coupons.  
\*minor  $\alpha$ -Al<sub>2</sub>O<sub>3</sub> from aluminum-air interaction.

Fig. 3. SEM images from the surface and core of unreacted and reacted NACM coupons.

### Tables

Table 1. Physical property changes of the coupons.

SAMPLE	Volume				Mass			
	Pre (cm <sup>3</sup> )	Post (cm <sup>3</sup> )	$\Delta$ (cm <sup>3</sup> )	% increase	Pre (g)	Post (g)	$\Delta$ (g)	% increase
<b>BRL-1 (300°C)</b>								
BRL-1-coupon1	1.58*	3.06	1.48	93.69	3.89 <sup>#</sup>	6.12	2.23	57.39
BRL-1-coupon2	1.58*	2.95	1.37	86.55	3.89 <sup>#</sup>	5.91	2.02	51.93
BRL-1-coupon3	1.58*	2.98	1.40	88.85	3.89 <sup>#</sup>	5.99	2.10	54.05
<b>Average</b>			<b>1.42</b>	<b>89.70</b>			<b>2.12</b>	<b>54.46</b>
<b>Standard Deviation</b>			<b>0.05</b>	<b>2.98</b>			<b>0.09</b>	<b>2.24</b>
<b>BRL-2 (150°C)</b>								
BRL-2-coupon1	1.59	1.63	0.04	2.63	4.01	4.07	0.06	1.57
BRL-2-coupon2	1.57	1.58	0.01	0.76	3.90	3.95	0.06	1.48
<b>Average</b>			<b>0.03</b>	<b>1.69</b>			<b>0.06</b>	<b>1.52</b>
<b>Standard Deviation</b>			<b>0.02</b>	<b>0.94</b>			<b>0.00</b>	<b>0.04</b>
<b>BRL-3 (230°C)</b>								
BRL-3-coupon1	1.61	1.72	0.11	6.59	3.96	4.11	0.15	3.85
BRL-3-coupon2	1.56	1.59	0.04	2.35	3.83	3.97	0.14	3.63
BRL-3-coupon3	1.63	1.69	0.06	3.93	4.02	4.17	0.15	3.75
<b>Average</b>			<b>0.07</b>	<b>4.29</b>			<b>0.14</b>	<b>3.69</b>
<b>Standard Deviation</b>			<b>0.03</b>	<b>1.75</b>			<b>0.01</b>	<b>0.06</b>

\*Estimated from average coupon dimension

<sup>#</sup>Calculated from the total mass of three coupons

# Hydrothermal reactivity of neutron absorber composites

Sauer et al.

## Supplemental Material

### S1. Methods

The Neutron Absorber Composite Material (NACM) used in this study was sourced from 3M Advanced Materials Division, Ceradyne, a 3M company. Hydrothermal experiments were conducted under fully saturated conditions in a flexible Au bag fixed to a titanium collar and head, enclosed in a titanium vessel following the experimental setup described in [11]. The vessel was pressurized to remain above water saturation pressure. The volumes of reaction cells used in the experiments were between 140 and 175 mL. The run conditions for the three experiments are listed in Table S1.

Table S1: Run conditions. Number in parentheses indicates number of coupons included in the experiment. NACM, Neutron Absorber Composite Material.

Exp.	Components	Temp. (°C)	Pressure (bar)	Run time
BRL-1	NACM (3) + DI	300	150	2 weeks
BRL-2	NACM (2) + DI	150	150	2 weeks
BRL-3	NACM (3) + DI	230	150	2 weeks

After experiment cooling, coupons were extracted from the vessels and dried. To observe the alteration mineralogy, coupons were mounted in a titanium sample holder so that the top of the coupon was even with the holder surface, thus providing a level area for a XRD scan. The Al surface of an unreacted NACM coupon was scanned with X-ray diffraction (XRD) to identify mineral phases in the starting materials. The core of an unreacted NACM coupon was exposed by filing away the aluminum cladding and analyzed by XRD. The reacted surface of each NACM coupon from the three experiments were analyzed in the same method described above. The cores of the coupons were similarly exposed by filing away the top surface and the XRD analysis was repeated. X-ray diffraction data was collected with a Siemens D500 diffractometer (Siemens, Munich, Germany) using Cu-K $\alpha$  radiation. Data were collected from 2 to 90 °2 $\theta$  with a 0.02 °2 $\theta$  step size and count times of 8 to 12 seconds per step. Mineral phases were identified using JADE® and the PDF-4 database.

Analytical electron microscopy was performed using a FEI™ Inspect F scanning electron microscope (SEM). Samples were not coated prior to SEM analysis. Imaging with the SEM was performed using a 15.0 kV accelerating voltage and 3.0 spot size.

Major cations and trace metals were analyzed via inductively coupled plasma-optical emission spectrometry (ICP-OES) (Optima 2100 DV, Perkin Elmer, Waltham, Massachusetts, USA) and inductively coupled plasma-mass spectrometry (ICP-MS) (Elan 6100, Perkin Elmer, Waltham, Massachusetts, USA) utilizing EPA methods 200.7 and 200.8 at Los Alamos National Laboratory. Ultra-high purity nitric acid was used in sample and calibration preparation prior to sample analysis. Internal standards (Sc for ICP-OES and Bi, In, and Y for ICP-MS) were added to samples and standards to correct for matrix effects. Standard Reference Material (SRM) 1643e Trace Elements in Water was used to check the accuracy of the multi-element calibrations.

Inorganic anion samples were analyzed by ion chromatography (IC) following EPA method 300 on a Dionex DX-600 system (Thermo, Waltham, Massachusetts, USA). Aqueous chemical results are presented in Appendix A. Typical two sigma uncertainties for the aqueous chemistry results are less than ~5%. The aqueous geochemical data for major cations and anions is presented in table S2.

## **S2. Characterization**

### **Physical changes**

The length, width, thickness, and mass of the reacted coupons was measured. Pre-experiment dimensions and masses for individual coupons was measured before BRL-2 and BRL-3. Individual coupon masses were not recorded before BRL-1; only the total mass of the three coupons was measured.

In BRL-1, the length and width of the coupons increased by ~4–8% whereas the thickness (i.e., height of the B<sub>4</sub>C-Al composite core plus aluminum cladding) increased by up to 60%. The combined coupon dimension changes resulted in a volume increase of around 90%. The masses of the coupons also increased by around 54%.

In comparison, the physical changes observed at 230 and 150°C were minimal. The length and width of the coupons from BRL-3 (230°C) slightly increased (~0.7–1.0% and ~0.0–2.3%, respectively). The thickness of the coupons increased by 0.0 to 0.01 cm, or 0.0–3.1%. The mass of each coupon increased by ~0.15 g (i.e., ~4%). At 150°C (BRL-2), the length, width, and thickness did not increase. Mass increase was about 0.06 g, or ~1.5%

The expansion of the coupons corresponded with a density decrease. The outward appearance of the aluminum cladding changed from shiny metal to matte grey or white powder. NAC coupons reacted at 300°C have a warped appearance; coupons are slightly thicker at the edges with a depression in the center (Fig. 1a).

### **SEM identification of mineral phases**

The cladding of unreacted Boral coupons displays a rough surface, characterized by parallel, thin striations (Fig. 2a). The core is characterized by B<sub>4</sub>C crystals (~50–250 µm) suspended in a fine-grained Al-sinter matrix.

In experiment BRL-1 (300°C), the SEM images show extensive alteration of the aluminum cladding to well-formed, crystalline boehmite (Fig. 3b). Boehmite crystals are up to ~25 µm in size and have a hexagonal crystal form. Boehmite formation is observed in the coupon composite core at 300°C, indicating alteration of Al sinter (Fig. 3f). Boehmite crystals in the core are generally finer grained than the crystals formed on the coupon surface.

Boehmite forms a thin coating on the surface of the aluminum cladding in the 230°C reacted coupons from BRL-3 (Fig 1). Boehmite crystals displays an elongate, hexagonal crystalline form and are ~1–5 µm in diameter (Fig. 3c). Alteration of aluminum to fine-grained boehmite is observed in the core material and potential dissolution pits were observed locally on boron carbide grains (Fig. 3g).

Pseudoboehmite forms a thin, poorly crystalline coating on the surface of the Al cladding in the 150°C reacted coupons from experiment BRL-2 (Fig. 3d). Boehmite crystals that are formed on the aluminum cladding are <1 µm and do not have a well-defined crystal form. Minor boehmite alteration is observed in the core material (Fig. 3h).

Table S2. Concentrations (mg/L) of major cations and anions in reaction fluids. F, filtered; UF, unfiltered.

Sample ID	Filter type	Time (hours)	pH	Anions							
				Bromide	Oxalate	Chloride	Fluoride	Nitrite	Nitrate	Phosphate	Sulfate
BRL-1 (300°C)											
BRL-1-1 UF Cat	UF	168	8.3	<0.1	<0.1	2.56	<0.1	<0.1	<0.1	<0.1	1.75
BRL-1-2 UF Cat	UF	336	8.0	<0.1	<0.1	2.79	<0.1	<0.1	<0.1	<0.1	1.29
BRL-2 (150°C)											
BRL-2-1 UF CAT	UF	168	6.1	<0.1	<0.1	0.42	0.26	<0.1	0.27	<0.1	1.99
BRL-2-2 UF CAT	UF	336	7.3	<0.1	<0.1	9.21	0.32	<0.1	0.21	<0.1	1.05
BRL-2-3 UF CAT	UF	360	6.2	<0.1	<0.1	0.16	0.21	<0.1	0.13	<0.1	1.26
BRL-1 (230°C)											
BRL-3-1 UF	UF	168	6.6	<0.1	<0.1	0.37	<0.1	<0.1	0.108	<0.1	0.63
BRL-3-2 UF	UF	336	6.2	<0.1	<0.1	0.52	<0.1	<0.1	<0.1	<0.1	0.58
BRL-3-3 UF	UF	360	7.2	<0.1	<0.1	0.54	<0.1	<0.1	0.1214	<0.1	0.91
Sample ID	Filter type	Time (hours)	pH	Cations							
				Al	B	Ba	Ca	Cr	Fe	K	Li
BRL-1 (300°C)											
BRL-1-1 F Cat	F	168	8.3	1.45	16.90	0.28	0.60	<0.006	0.06	<1.122	0.03
BRL-1-2 F Cat	F	336	8.0	1.99	18.75	<0.022	0.17	<0.006	0.07	<1.122	0.03
BRL-1-1 UF Cat	UF	168	8.3	2.22	17.11	0.04	0.62	<0.006	<0.036	<1.122	0.04
BRL-1-2 UF Cat	UF	336	8.0	1.17	18.70	0.11	0.52	<0.006	0.16	<1.122	0.04
BRL-2 (150°C)											
BRL-2-1 F CAT	F	168	6.1	<0.032	14.96	0.07	0.49	0.01	0.10	3.46	0.02
BRL-2-2 F CAT	F	336	7.3	0.04	15.29	0.67	1.21	0.01	0.18	1.42	<0.012
BRL-2-3 F CAT	F	360	6.2	<0.032	15.15	0.05	0.30	0.01	0.10	<1.122	<0.012
BRL-2-1 UF CAT	UF	168	6.1	0.08	15.35	0.09	0.55	0.01	0.11	2.10	0.02
BRL-2-2 UF CAT	UF	336	7.3	0.04	15.00	0.10	0.60	0.01	0.09	1.29	<0.012
BRL-2-3 UF CAT	UF	360	6.2	2.56	15.04	0.04	0.31	<0.006	0.10	<1.122	<0.012
BRL-1 (230°C)											
BRL-3-1 F	F	168	6.6	0.39	14.26	<0.022	0.40	<0.006	<0.036	<1.122	<0.012
BRL-3-2 F	F	336	6.2	0.36	14.23	<0.022	0.47	<0.006	<0.036	<1.122	0.01
BRL-3-3 F	F	360	7.2	0.44	13.74	<0.022	0.44	<0.006	<0.036	<1.122	0.01
BRL-3-1 UF	UF	168	6.6	0.23	14.68	<0.022	0.54	<0.006	<0.036	<1.122	<0.012
BRL-3-2 UF	UF	336	6.2	0.45	15.14	<0.022	0.66	<0.006	0.04	<1.122	0.02
BRL-3-3 UF	UF	360	7.2	0.07	14.16	<0.022	0.35	<0.006	<0.036	<1.122	0.02
BRL-1 (300°C)											
BRL-1-1 F Cat	F	168	8.3	<0.02	<0.006	5.02	17.27	36.97	0.01	<0.004	<0.104
BRL-1-2 F Cat	F	336	8.0	<0.02	<0.006	5.70	12.80	27.38	<0.0008	0.01	<0.104
BRL-1-1 UF Cat	UF	168	8.3	<0.02	<0.006	4.97	19.55	41.83	0.01	0.00	<0.104
BRL-1-2 UF Cat	UF	336	8.0	<0.02	<0.006	5.58	11.93	25.52	0.01	0.04	0.20
BRL-2 (150°C)											
BRL-2-1 F CAT	F	168	6.1	0.46	<0.006	4.60	1.53	3.27	0.00	<0.004	<0.104
BRL-2-2 F CAT	F	336	7.3	0.47	0.01	<2.498	2.15	4.61	0.02	<0.004	<0.104
BRL-2-3 F CAT	F	360	6.2	0.67	0.01	<2.498	0.80	1.71	0.00	<0.004	<0.104
BRL-2-1 UF CAT	UF	168	6.1	0.51	0.01	3.31	1.71	3.65	0.00	<0.004	<0.104
BRL-2-2 UF CAT	UF	336	7.3	0.50	0.01	<2.498	1.59	3.41	0.01	<0.004	<0.104
BRL-2-3 UF CAT	UF	360	6.2	0.71	<0.006	<2.498	0.67	1.43	0.00	<0.004	<0.104
BRL-1 (230°C)											
BRL-3-1 F	F	168	6.6	0.03	<0.006	<2.498	<0.556	<1.18984	0.00	<0.004	<0.104
BRL-3-2 F	F	336	6.2	0.06	<0.006	<2.498	<0.556	<1.18984	0.00	<0.004	<0.104
BRL-3-3 F	F	360	7.2	0.08	<0.006	<2.498	<0.556	<1.18984	0.00	<0.004	<0.104
BRL-3-1 UF	UF	168	6.6	0.07	<0.006	<2.498	<0.556	<1.18984	0.00	<0.004	0.14
BRL-3-2 UF	UF	336	6.2	0.04	<0.006	<2.498	<0.556	<1.18984	0.00	<0.004	<0.104
BRL-3-3 UF	UF	360	7.2	0.07	<0.006	<2.498	<0.556	<1.18984	0.00	<0.004	<0.104



